

This work was written as part of one of the author's official duties as an Employee of the United States Government and is therefore a work of the United States Government. In accordance with 17 U.S.C. 105, no copyright protection is available for such works under U.S. Law. Access to this work was provided by the University of Maryland, Baltimore County (UMBC) ScholarWorks@UMBC digital repository on the Maryland Shared Open Access (MD-SOAR) platform.

Please provide feedback

Please support the ScholarWorks@UMBC repository by emailing scholarworks-group@umbc.edu and telling us what having access to this work means to you and why it's important to you. Thank you.

Optical vortices during a superresolution process in a metamaterial

G. D'Aguanno,^{1,*} N. Mattiucci,¹ M. Bloemer,¹ and A. Desyatnikov²

¹Research, Development, and Engineering Command, Department of the Army, Charles M. Bowden Facility, Building 7804, Redstone Arsenal, Alabama 35898, USA

²Nonlinear Physics Centre, Research School of Physical Sciences and Engineering, Australian National University, Canberra, Australian Capital Territory 0200, Australia

(Received 3 December 2007; published 17 April 2008)

We show that a superresolution process with 100% visibility is characterized by the formation of a point of phase singularity in free space outside a metamaterial in the form of a saddle with topological charge equal to -1 . The saddle point is connected to two vortices at the end boundaries of the lens, and the two vortices are in turn connected to another saddle point inside the lens. The structure saddle-vortices-saddle is topologically stable. The formation of the saddle point in free space explains also the negative flux of energy present in a certain region of space outside the lens. The circulation strength of the power flow can be controlled by varying the position of the object plane with respect to the lens.

DOI: [10.1103/PhysRevA.77.043825](https://doi.org/10.1103/PhysRevA.77.043825)

PACS number(s): 42.25.Fx, 42.30.Va

Vortices are ubiquitous in nature from the macroscopic to the microscopic world. Tornados and hurricanes [1] or whirlpools [2] are maybe the most common examples at macroscopic distances. At micrometer scales, vortices have been observed in superfluid He II [3] and in a Bose-Einstein condensate of ⁸⁷Rb atoms [4,5]. In optics, vortices have been observed in the near field diffracted by an array of subwavelength apertures [6–9], in lasers [10], in optical fibers or in systems that create caustics or speckle fields [11], with the help of computer generated holograms [12] and spiral phase plates [13], and in nonlinear media [14,15] including quadratic materials [16]. Their applications include free space interconnection of electronic components [17], optical trapping of viruses and bacteria [18] as well as small particles [19], quantum information and quantum cryptography [20,21], fluorescence microscopy with nanoscale resolution [22], and extrasolar planet detection [23,24]. Optical vortices are based on the appearance of phase singularities (also called “phase dislocations”) whenever the field intensity vanishes, as pointed out in the seminal paper by Nye and Berry [25].

Let us consider for simplicity the expression of the time-averaged Poynting vector for a monochromatic field in a two-dimensional geometry: $\vec{S}(x, z) = (1/2)\text{Re}[\vec{E}(x, z) \times \vec{H}^*(x, z)]$ where $\vec{E}(x, z)$ and $\vec{H}(x, z)$ are the complex amplitudes of the electric and magnetic fields, respectively. The phase of the Poynting vector can be extracted from its components through the following equations: $\sin \Phi_S(x, z) = S_z(x, z) / |\vec{S}(x, z)|$ and $\cos \Phi_S(x, z) = S_x(x, z) / |\vec{S}(x, z)|$. Now, if we assume that at some point in space $|\vec{S}(x, z)| = 0$ (black spot), then the phase of the Poynting vector will be, of course, not defined (singular) at that point and in its neighborhood there can be three possible situations: (a) a left-handed or right-handed circular power flow (optical vortex), (b) a power flow in the form of a source or

sink, or (c) a power flow in the form of a saddle [25,26]. Obviously, in free space a power flow in the form of a source or a sink is excluded. Due to the appearance of those phase singularities, the branch of optics that studies vortices is usually referred to as “singular optics,” and singular optics is emerging as a new and exciting chapter of modern optics [27]. A quantity that is useful in the study of optical vortices is the so-called topological charge which can be defined for the Poynting vector as [28] $s = (1/2\pi) \oint_C \vec{\nabla} \Phi_S \cdot d\vec{r}$, where the path integral is taken counterclockwise along any closed line C surrounding the point of phase singularity. The topological charge is in general an integer number because the phase varies by multiples of 2π around the singular point, and it counts the algebraic number of phase jumps along the closed line C associated with the helical structure of Φ_S .

In the past few years, negative index materials (NIMs), i.e., materials that have simultaneously negative permittivity (ϵ) and permeability (μ), have been the subject of intense theoretical and experimental investigations [29,30]. One of the most important applications is the possibility of using them to construct a “perfect” lens, i.e., a lens that can also focus the evanescent near-field components of an object, as pointed out by Pendry several years ago in his seminal paper [29]. In 2005 the first NIMs operating in the visible regime were reported [31,32] and shortly after a silver-based NIM operating at telecommunication wavelengths was theoretically studied [33] and experimentally realized [34]. One serious issue that is detrimental for achievement of a superresolving lens is the fact that in currently available metamaterials the absorption or scattering losses are still very high. A much simpler superresolving lens can be obtained by using one-dimensional metallodielectric multilayer structures [35–38] in which low-group-velocity surface plasmon modes are excited for TM polarization of the light. Those metallodielectric lenses have only the permittivity (ϵ) negative due to the presence of the metal layers, and therefore they mimic a NIM only for TM polarization of the light [35–39]; nevertheless, they retain many salient characteristics of a true NIM as regards superresolution purposes, and, more important, they have the advantage of low losses in the

*Corresponding author. FAX: 001-256-8422507. giuseppe.daguanno@us.army.mil; giuseppe.daguanno@gmail.com

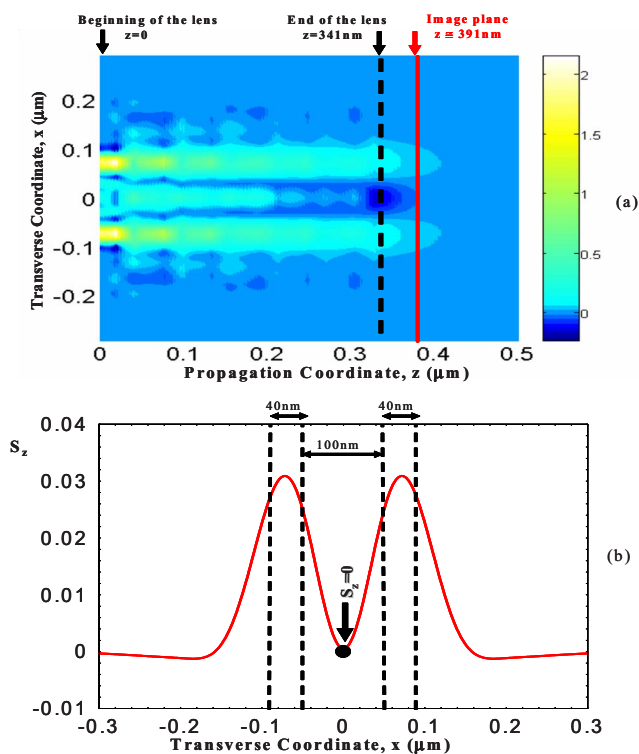


FIG. 1. (Color online) (a) S_z (arbitrary units) in the x - z plane. The dashed (continuous) line indicates the position of the end of the lens (the image plane). (b) Section of S_z at the image plane ($z \cong 391$ nm) where 100% visibility is achieved. Superimposed dashed lines indicate the positions of the two slits.

visible range. We would like to point out that here we are in a situation where the distance between the image plane and the object plane is one wavelength or less, i.e., we are in the near field; these distances are typical for the study of super-resolution [29,35,36,39]. It is worth mentioning that a lens that seems promising in achieving superresolution in the far field has also been proposed [40]. Superresolution in the far field is usually referred to as “hyperresolution” and the lens that achieves it is called a hyperlens.

In a recent publication [39], we have shown that broadband superresolution can be achieved in a metallodielectric lens made of 5.5 periods of Ag/GaP (22 nm/35 nm) with 17-nm-thick GaP antireflection coatings on the entrance and exit faces for a total length $L=341$ nm. The lens maintains a good transparency ($\sim 60\%$ of the input power is transmitted by the lens) over the superresolving range 500–650 nm. For an incident wavelength of 532 nm, the lens is able to resolve two slits (40 nm wide with center to center distance of 140 nm) with 100% visibility at 50 nm beyond the end face of the lens. The slits are placed at the entrance of the lens (but in free space). In Fig. 1(a) we show $S_z(x,z)$ during the superresolution process and in Fig. 1(b) we show $S_z(x,z \cong 391$ nm) where the visibility approaches 100%. The black spot indicates the point of coordinates $(x=0, z \cong 391$ nm) where $S_z=0$. At points in the vicinity of $x=0, z \cong 391$ nm, $S_z \neq 0$. Figure 2(a) shows that not only $S_z=0$ but also $S_x=0$ at the point $(x=0, z \cong 391$ nm) and therefore we can expect the presence of a point of phase singularity around this point (black spot). In Fig. 2(b) we

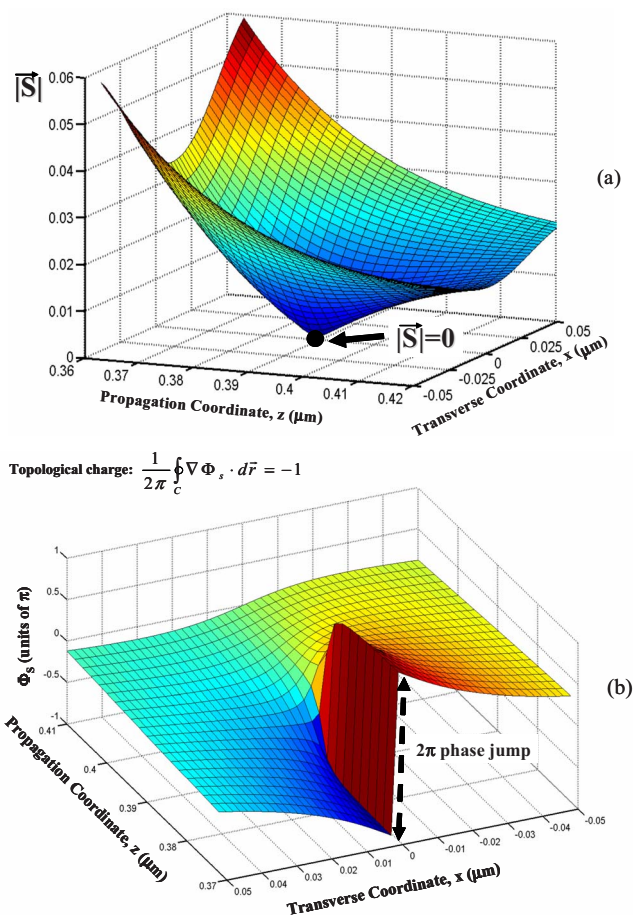


FIG. 2. (Color online) (a) Three-dimensional plot of $|\vec{S}| = \sqrt{S_x^2 + S_z^2}$ in the x - z plane in a small region around the black spot. (b) Structure of the phase of the Poynting vector (Φ_S) around the black spot.

show the phase Φ_S around the black spot. In this case we have just one phase jump of 2π along a closed line C surrounding the black spot and therefore the topological charge is $s=-1$ when C is oriented counterclockwise. In Fig. 3 we show the vector field \vec{S} around the black spot. The black spot is a saddle point and the power flow is characterized by four perfectly symmetric regions of circulation. The energy is flowing toward the black spot along the x direction, while it is flowing away from the black spot along the z direction. Note that the flux of energy is negative in the region of free space delimited by the boundaries ($z_{\min} \cong 341$ nm, $z_{\max} \cong 391$ nm, $x_{\min} \cong -18$ nm, $x_{\max} \cong 18$ nm). A negative flux of energy in free space may appear counterintuitive, but is instead perfectly explained by the formation of the saddle point at $(x=0, z \cong 391$ nm). This negative flux of energy has also been reported in Ref. [41], although there it was ascribed to the finite transverse dimension of the lens, while it is clear now that it is due to the formation of a saddle point. The strength of the circulation of the power flow in air and the position of the saddle point can be controlled by varying a , i.e., the distance of the object plane with respect to the input face of the lens. In particular, the position of the black spot becomes closer to the end of the lens and at the

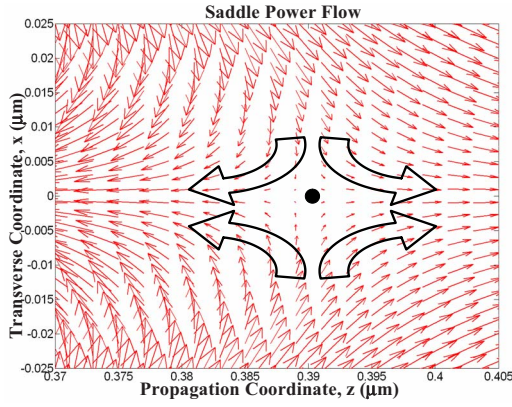


FIG. 3. (Color online) Vector field \vec{S} (little arrows) in a small region around the saddle point (black spot). The big arrows are shown to help the eye. For a better view the magnitude of the Poynting vector has been magnified ten times with respect to the values reported in Figs. 1 and 2(a).

same time the strength of the circulation of the power flow decreases when the distance between the object plane and the beginning of the lens increases. We have also calculated the diffraction from the two slits in free space (i.e., without the metallodielectric lens in place). In this case there is no saddle point on the z axis at $x=0$ and no negative energy flux. Therefore, the onset of the saddle point must be ascribed to the presence of the superlens and to the fact that 100% visibility is achieved. In Fig. 4 we show the circulation of the Poynting vector $(\vec{\nabla} \times \vec{S})_y$ [42] in free space at $z \cong 343$ nm (i.e., in free space immediately after the end of the lens) as a function of a , by varying a in steps of 10 nm. As we will see in a moment, the peaks and the valleys of the circulation are related, respectively, to the presence of left-handed (LVs) and right-handed (RVs) vortices at the boundary of the lens.

Usually the saddle must be connected to other dislocations, and in fact in Fig. 5 we show that the saddle point (S1) in our case is connected to two vortices, left-handed (LV1) and right handed (RV1), respectively, which are centered at the last Ag/GaP interface in a symmetric position with

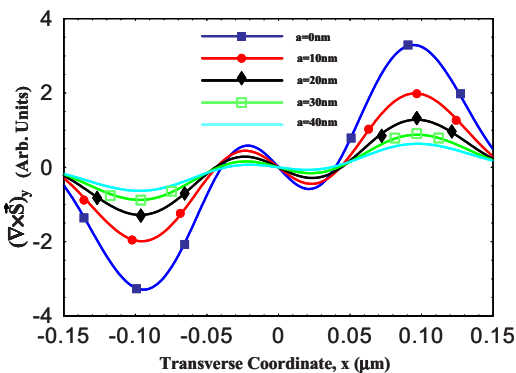


FIG. 4. (Color online) $(\vec{\nabla} \times \vec{S})_y$ (arbitrary units) vs x (micrometers) at $z \cong 343$ nm for different distances a of the object plane from the input surface of the lens.

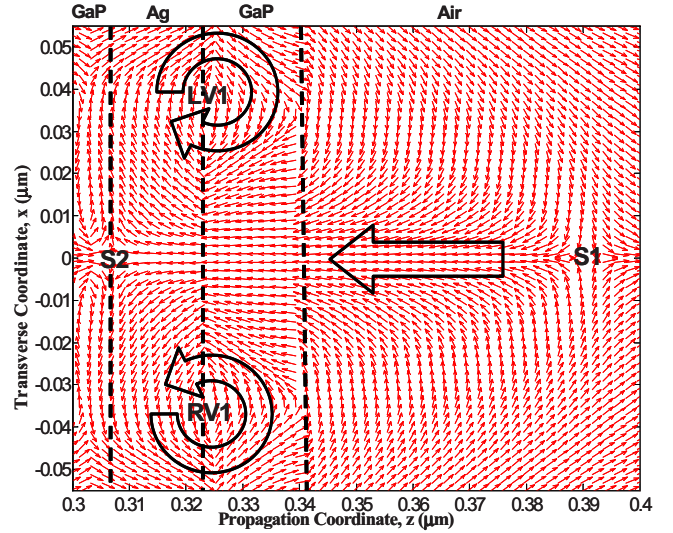


FIG. 5. (Color online) Arrow representation of the unit vector $\vec{S}/|\vec{S}|$. The saddle point (S1) is connected to two vortices, right-handed (RV1) and left-handed (LV1), respectively, centered at the last Ag/GaP interface. These vortices are in turn connected to a second saddle point (S2) inside the lens centered at the penultimate GaP/Ag interface. The big arrows sketch the flux of the energy. Note in particular the negative flux of energy directed toward the end of the lens.

respect to the saddle point. The two vortices are in turn connected to another saddle point (S2) inside the lens. The structure S1-LV1-RV1-S2 is a manifestation of the superresolution process with 100% visibility. In order to address the issue of the topological stability of the structure, we calculate the Poynting vector outside the lens in the case of two slightly asymmetric slits. The first slit is now positioned between $x_{1-} = -100$ nm and $x_{1+} = -50$ nm (therefore the width of the slit is now 50 nm instead of 40 nm) while the position and the width of second slit remain unchanged. The calculations show that the structure S1-LV1-RV1-S2 remains practically unchanged with just a slight modification in its location, proving therefore the topological stability. We would like to underline that in this work we have focused our attention only on the structure S1-LV1-RV1-S2, which characterizes the superresolution with 100% visibility. As a matter of fact, the structure of the phase dislocations inside the superlens is much more complicated and far richer, although a detailed mapping of all the phase dislocations is outside the scope of the present work. The calculations presented here have been performed using the angular spectrum representation technique [43] in conjunction with a matrix transfer technique [44]. The method, given its intrinsic analytical nature, avoids any numerical problems. The same technique has also been successfully applied in Ref. [45] to study the influence of losses on the superresolution capabilities of an impedance-matched negative index material.

In conclusion, we have demonstrated that a superresolution process with 100% visibility is accompanied by the formation of a structure S1-LV1-RV1-S2 which is topologically stable. We expect that our findings may have important applications in the field of optical interconnections at the

nanoscale level, optical trapping of viruses and bacteria, and optical trapping of particles. We hope also that our results may stimulate the finding of further connections between the fascinating fields of singular optics and metamaterials.

G.D. and A.D. thank Yuri Kivshar for helpful discussions. The research of G.D. and N.M. is supported by the National Research Council of the United States; the research of A.D. is supported by the Australian Research Council.

-
- [1] K. Emanuel, *Divine Wind: The History and Science of Hurricanes* (Oxford University Press, New York, 2005).
- [2] G. Gjevik, H. Moe, and A. Ommundsen, *Nature (London)* **388**, 837 (1997).
- [3] E. L. Andronikashvili and Yu. G. Mamaladze, *Rev. Mod. Phys.* **38**, 567 (1966).
- [4] M. H. Anderson *et al.*, *Science* **269**, 198 (1995).
- [5] J. E. Williams and M. J. Holland, *Nature (London)* **401**, 568 (1999).
- [6] T. W. Ebbesen *et al.*, *Nature (London)* **391**, 667 (1998).
- [7] T. Thio *et al.*, *Opt. Lett.* **26**, 1972 (2001).
- [8] H. F. Schouten *et al.*, *Opt. Express* **11**, 371 (2003).
- [9] H. F. Schouten, T. D. Visser, D. Lenstra, and H. Blok, *Phys. Rev. E* **67**, 036608 (2003).
- [10] A. B. Coates *et al.*, *Phys. Rev. A* **49**, 1452 (1994).
- [11] *Optical Vortices*, edited by M. Vasnetsov and K. Staliunas, Horizons in World Physics Vol. 228 (Nova Science, New York, 1999).
- [12] J. Arlt, K. Dholokia, L. Allen, and M. J. Padgett, *J. Mod. Opt.* **45**, 1231 (1998).
- [13] M. W. Beijersbergen, R. P. C. Coerwinkel, M. Kristensen, and J. P. Woerdman, *Opt. Commun.* **112**, 321 (1994).
- [14] V. Tikhonenko, J. Christou, B. Luther-Davis, and Yu. S. Kivshar, *Opt. Lett.* **21**, 1129 (1996); Yu. S. Kivshar and E. A. Ostrovskaya, *Opt. Photonics News*, **12**, 27 (2001).
- [15] Yu. S. Kivshar and D. E. Pelinovsky, *Phys. Rep.* **331**, 117 (2000); A. S. Desyatnikov, Yu. S. Kivshar, and L. Torner, in *Progress in Optics*, edited by E. Wolf (Elsevier, Amsterdam, 2005), Vol. 47, pp. 291–391.
- [16] P. Di Trapani, W. Chinaglia, S. Minardi, A. Piskarskas, and G. Valiulis, *Phys. Rev. Lett.* **84**, 3843 (2000).
- [17] J. Scheuer and M. Orenstain, *Science* **285**, 230 (1999).
- [18] A. Ashkin and J. M. Dziedzic, *Science* **235**, 1517 (1987).
- [19] K. T. Gahagan and G. A. Swartzlander, *J. Opt. Soc. Am. B* **16**, 533 (1999).
- [20] A. Mair, A. Vaziri, G. Weihs, and A. Zeilinger, *Nature (London)* **412**, 313 (2001).
- [21] H. H. Arnaut and G. A. Barbosa, *Phys. Rev. Lett.* **85**, 286 (2000).
- [22] V. Westphal and S. W. Hell, *Phys. Rev. Lett.* **94**, 143903 (2005).
- [23] J. H. Lee, G. Foo, E. G. Johnson, and G. A. Swartzlander, Jr., *Phys. Rev. Lett.* **97**, 053901 (2006).
- [24] F. Tamburini, G. Anzolin, G. Umbricco, A. Bianchini, and C. Barbieri, *Phys. Rev. Lett.* **97**, 163903 (2006).
- [25] J. F. Nye and M. V. Berry, *Proc. R. Soc. London, Ser. A* **336**, 165 (1974).
- [26] J. F. Nye, *Natural Focusing and the Fine Structure of Light* (Institute of Physics, Bristol, 1999).
- [27] M. S. Soskin and M. V. Vasnetsov, in *Progress in Optics*, edited by E. Wolf (Elsevier, Amsterdam, 2001), Vol. 42, pp. 219–276.
- [28] In our analysis we are interested in the study of the Poynting vector because it gives the actual direction of the power flow. A topological charge for the “phase” of the real vector field here is defined similarly to the usual definition for the phase of a scalar complex electric field.
- [29] J. B. Pendry, *Phys. Rev. Lett.* **85**, 3966 (2000), and references therein.
- [30] R. A. Shelby, D. R. Smith, and S. Schultz, *Science* **292**, 77 (2001).
- [31] S. Zhang, W. Fan, N. Panoiu, K. Malloy, R. Osgood, and S. Brueck, *Phys. Rev. Lett.* **95**, 137404 (2005).
- [32] V. M. Shalaev *et al.*, *Opt. Lett.* **30**, 3356 (2005).
- [33] S. Zhang *et al.*, *Opt. Express* **13**, 4922 (2005).
- [34] G. Dolling *et al.*, *Opt. Lett.* **31**, 1800 (2006).
- [35] S. A. Ramakrishna, J. B. Pendry, M. C. K. Wiltshire, and W. J. Stewart, *J. Mod. Opt.* **50**, 1419 (2003).
- [36] H. Shin and S. Fan, *Appl. Phys. Lett.* **89**, 151102 (2006).
- [37] B. Wood, J. B. Pendry, and D. P. Tsai, *Phys. Rev. B* **74**, 115116 (2006).
- [38] K. J. Webb and M. Yang, *Opt. Lett.* **31**, 2130 (2006).
- [39] M. J. Bloemer *et al.*, *Appl. Phys. Lett.* **90**, 174113 (2007).
- [40] Z. Liu *et al.*, *Science* **315**, 1686 (2007), and references therein.
- [41] L. Chen, S. He, and L. Shen, *Phys. Rev. Lett.* **92**, 107404 (2004).
- [42] K. J. Webb and M.-C. Yang, *Phys. Rev. E* **74**, 016601 (2006).
- [43] L. Mandel and E. Wolf, *Optical Coherence and Quantum Optics* (Cambridge University Press, Cambridge, U.K., 1995).
- [44] A. Yariv and P. Yeh, *Optical Waves in Crystals* (Wiley, New York, 1984).
- [45] G. D’Aguanno, N. Mattiucci, and M. J. Bloemer, *J. Opt. Soc. Am. B* **25**, 236 (2008).